



**HAL**  
open science

## Quasi-neutrality equation in a polar mesh

Christophe Steiner, Michel Mehrenberger, Nicolas Crouseilles, Philippe Helluy

► **To cite this version:**

Christophe Steiner, Michel Mehrenberger, Nicolas Crouseilles, Philippe Helluy. Quasi-neutrality equation in a polar mesh. 2015. hal-01248179

**HAL Id: hal-01248179**

**<https://hal.science/hal-01248179>**

Preprint submitted on 24 Dec 2015

**HAL** is a multi-disciplinary open access archive for the deposit and dissemination of scientific research documents, whether they are published or not. The documents may come from teaching and research institutions in France or abroad, or from public or private research centers.

L'archive ouverte pluridisciplinaire **HAL**, est destinée au dépôt et à la diffusion de documents scientifiques de niveau recherche, publiés ou non, émanant des établissements d'enseignement et de recherche français ou étrangers, des laboratoires publics ou privés.

# Quasi-neutrality equation in a polar mesh<sup>1</sup>

Christophe Steiner \*    Michel Mehrenberger \*    Nicolas Crouseilles †  
Philippe Helluy \*

December 24, 2015

## Abstract

In this work, we are concerned with the numerical resolution of the quasi-neutrality equation arising in plasma physics. A classic method is based on a Padé approximation. Two other methods are proposed in this paper: a Padé approximation of higher order and a direct method in the space configuration which consists in integrating on the gyrocircles using interpolation operator. Numerical comparisons are performed with analytical solutions and considering the  $4D$  drift-kinetic model with one Larmor radius. This is a preliminary study; further study in GYSELA is envisioned.

## 1 Introduction

In strongly magnetized plasma, when collisions are not the dominant collective effect, one has to deal with kinetic models. Fluid models, which assume that the distribution function is close to an equilibrium, are no more suitable. However, the numerical solution of Vlasov type models is challenging since this model involves six dimensions in the phase space. Moreover, multi-scaled phenomena make the problem very difficult. Gyrokinetic theory enables to get rid of one of these constraints since the explicit dependence on the phase angle of the Vlasov equation is removed through gyrophase averaging while gyroradius effects are retained. The so-obtained five-dimensional function should be self-consistently coupled with Maxwell equations. In the following we consider the electrostatic approximation, where Maxwell equations are reduced to a Poisson equation (or its asymptotic counterpart, the so-called quasi-neutrality equation). The work presents here will still be applicable taking into account electromagnetic effects.

The present work is devoted to the numerical resolution of the quasi-neutrality equation in a polar mesh which is the framework in the gyrokinetic code GYSELA [15, 16]. We propose two alternatives to the classic Padé approximation by using *(i)* a Padé approximation of higher order or *(ii)* a direct method in the space configuration using interpolation operator.

---

\*INRIA Nancy-Grand Est (TONUS Project) and IRMA Strasbourg

†INRIA Rennes-Bretagne Atlantique

<sup>1</sup>This work has been carried out within the framework of the EUROfusion Consortium and has received funding from the Euratom research and training programme 2014-2018 under grant agreement N° 633053. The views and opinions expressed herein do not necessarily reflect those of the European Commission.

The paper is organized as follows. In Section 2, we introduce the quasi-neutrality equation in the gyrokinetic framework. The numerical methods are described in Section 3 for the classic and new Padé approximations and in Section 4 for the method based on interpolation. These methods will be applied to gyrokinetic simulations in Section 5.

## 2 Quasi-neutrality equation in the gyrokinetic framework

The computational effort to numerically solve the 6 dimensional Vlasov-Maxwell systems which describes plasma turbulence in tokamak plasmas still remains out of reach for present day supercomputers. All the numerical simulations performed until now in this domain take care of the gyrokinetic ordering to reduce this problem of one dimension. This ordering takes into account the fact that (i) electromagnetic fluctuations occur on time scales much longer than charged particle gyration period ( $\omega/\Omega_c \ll 1$  with  $\omega$  the fluctuation frequency and  $\Omega_c$  the cyclotron frequency), and (ii) the wavelength of these fluctuations is much smaller than the characteristic scale length of the gradients of magnetic field, density and temperature. See [14] for a detailed review on the gyrokinetic framework and simulations to compute turbulent transport in fusion plasmas. Within this gyro-ordering, the so-called gyrokinetic model can be derived (see [26]) by averaging on the fast gyration of charged particles around the magnetic field lines. The magnetic toroidal configuration considered in this paper is simplified. Indeed, magnetic flux surfaces are assumed concentric tori with circular cross-sections. The gyroaverage operator occurs in this reduction from 6 to 5 dimensions. The new 5D set of coordinates corresponds to: (i) 3D toroidal spatial coordinates  $(r, \theta, \varphi)$  (with  $r$  the radial direction,  $\theta$  and  $\varphi$  the poloidal (resp. toroidal) angle), and (ii) 2D in velocity space with  $v_{\parallel}$  the velocity parallel to the magnetic field line and  $\mu = m|v_{\perp}|^2/(2B)$  the magnetic moment where  $v_{\perp}$  represents the velocity in the plane orthogonal to the magnetic field of amplitude  $|B|$ . It is important to note that in this ordering  $\mu$  is an adiabatic invariant, so it plays the role of a parameter in the 5D gyrokinetic Vlasov equation.

In the following, the 4D problem which is treated corresponds to the case where we consider a unique value of  $\mu$ , *i.e.* the same Larmor radius is taken for all particles.

$T_i$ ,  $T_e$  and  $n_0$  refer to ion temperature, electron temperature and density profiles and will be defined at the beginning of Section 5. Numerical solutions are computed using normalized equations. The temperature is normalized to  $T_{e0}$ , where  $T_{e0}$  is defined by the initial temperature profile such that  $T_e(r_p)/T_{e0} = 1$  where  $r_p \in [r_{\min}, r_{\max}]$  is the radial coordinate of the peak of the initial distribution function. The time is normalized to the inverse of the ion cyclotron frequency  $\omega_c = e_i B_0/m_i$ . Velocities, including the parallel velocity, are expressed in units of the ion speed  $v_{T0} = \sqrt{T_{e0}/m_i}$ , the electric potential is normalized to  $T_{e0}/e_i$  and the magnetic field is normalized to  $B_0$ . Consequently, lengths are normalized to the Larmor radius  $\rho = m_i v_{T0}/e_i B_0$  and the magnetic moment  $\mu$  to  $T_{e0}/B_0$ .

The time evolution of the gyrocenter distribution function  $f$  is given by the gyrokinetic conservative equation (see also Eqs (17)-(20) in [14]):

$$B_{\parallel}^* \frac{\partial f}{\partial t} + \nabla \cdot \left( B_{\parallel}^* \frac{d\mathbf{x}_G}{dt} f \right) + \frac{\partial}{\partial v_{G\parallel}} \left( B_{\parallel}^* \frac{dv_{G\parallel}}{dt} f \right) = 0 \quad (2.1)$$

where  $\mathbf{x}_G$  and  $v_{G\parallel}$  are respectively the space coordinates and the parallel velocity of the guiding centers. In the electrostatic limit, for a particle of mass  $m$  and charge  $q$  the motion equations of the guiding centers are given by

$$\frac{d\mathbf{x}_G}{dt} = v_{G\parallel}\mathbf{b}^* + E \times B + \mathbf{v}_D \quad (2.2)$$

$$m \frac{dv_{G\parallel}}{dt} = -\mu \nabla_{\parallel}^* B - q \nabla_{\parallel}^* \bar{\Phi} + mv_{G\parallel} E \times B \cdot \frac{\nabla B}{B} \quad (2.3)$$

where  $\nabla_{\parallel}^* \equiv \mathbf{b}^* \cdot \nabla$ , while  $\mathbf{b}^*$  and  $B_{\parallel}^*$  are defined by:

$$\mathbf{b}^* \equiv \frac{\mathbf{B}}{B_{\parallel}^*} + \frac{mv_{G\parallel}}{qB_{\parallel}^*B} \nabla \times \mathbf{B} \quad (2.4)$$

$$B_{\parallel}^* \equiv B + \frac{mv_{G\parallel}}{qB} \mathbf{b} \cdot (\nabla \times \mathbf{B}). \quad (2.5)$$

The drift reads  $E \times B = (1/B_{\parallel}^*)\mathbf{b} \times \nabla \bar{\Phi}$  while curvature drift is defined as  $\mathbf{v}_D = \left( \frac{mv_{G\parallel}^2 + \mu B}{qB_{\parallel}^*} \right) \mathbf{b} \times \frac{\nabla B}{B}$ .

The obtained function in five dimensions must be self-consistent coupled with Maxwell's equations. In the following, we consider the electrostatic approximation, where Maxwell's equations are reduced to a quasi-neutrality equation which is asymptotically equivalent to the Poisson equation. Since the Poisson equation is defined on the particles coordinates, the resolution of the gyrokinetic Vlasov-Poisson system requires an operator which transforms the gyrocentered phase space to the particles phase space. Let  $\vec{\rho}$  be the gyro-radius which is transverse to  $\mathbf{b}$  and which depends on the gyrophase  $\alpha \in [0, 2\pi]$ , *i.e.*

$$\vec{\rho} = \rho(\cos(\alpha)\vec{e}_{\perp 1} + \sin(\alpha)\vec{e}_{\perp 2}).$$

Here  $\vec{e}_{\perp 1}$  and  $\vec{e}_{\perp 2}$  are the unit vectors of a cartesian basis in the plane perpendicular to the magnetic field direction  $\mathbf{b}$ . Let  $\vec{x}_G$  be the guiding-center radial coordinate and  $\vec{x}$  the position of the particle in the real space. These two quantities differ by a Larmor radius  $\vec{\rho}$ , *i.e.*  $\vec{x} = \vec{x}_G + \vec{\rho}$ . Let  $f : (r, \theta) \in \mathbb{R}^+ \times \mathbb{R} \mapsto f(r, \theta)$  be a polar function and  $g : (x_1, x_2) \in \mathbb{R}^2 \mapsto g(x_1, x_2)$  the function defined by  $g(r \cos(\theta), r \sin(\theta)) = f(r, \theta)$  for all  $(r, \theta)$ . The function  $f$  (resp.  $g$ ) stands for field quantity defined on  $\vec{x}$  with polar (resp. cartesian) coordinates. The gyroaverage  $\mathcal{J}_{\rho}(f)$  of  $f$  depending on the spatial coordinates is defined as

$$\mathcal{J}_{\rho}(f)(r, \theta) = \frac{1}{2\pi} \int_0^{2\pi} g(\vec{x}_G + \vec{\rho}) d\alpha$$

where  $\vec{x}_G = r(\cos(\theta), \sin(\theta))$ . This gyroaverage process consists in computing an average on the Larmor circle. It tends to damp any fluctuation which develops at sub-Larmor scales. This operator is studied in [35] and we also refer to an abundant literature on this subject (see [5, 19, 28] and references in these articles).

The gyroaveraged electrostatic potential is solution of the self-consistently coupled 3D quasi-neutrality equation:

$$\frac{n_0(r)}{T_i(r)} \int_{\mathbb{R}^+} (\Phi - \mathcal{J}_{\sqrt{2\mu T_i}}^2(\Phi)) \exp(-\mu) d\mu + \frac{n_0(r)}{T_e(r)} (\Phi - \lambda \langle \Phi \rangle) = \bar{n}_i - n_0(r). \quad (2.6)$$

$\lambda$  is an integer which is expand to 0 or 1 according to the fact that zonal flows are taken into account or not.

We consider a simplified model of the system of equations (2.1)-(2.6). A periodic cylindrical plasma of radius  $a$  and length  $2\pi R$  (with  $R$  the major radius) is considered as a limit case of a stretched torus. The plasma is confined by a strong magnetic which is uniform  $\mathbf{B} = B\mathbf{e}_z$  where  $\mathbf{e}_z$  stand for the unit vector in the toroidal direction  $z$ . With these assumptions the velocity drifts are reduced to the  $\mathbf{E} \times \mathbf{B}$  drift. This SLAB 4D case is equivalent to the one treated in [24] or [15]. The equation satisfied by the distribution function of ions  $f(t, r, \theta, z, v)$  following the guiding center movement reads:

$$\begin{aligned} \partial_t f - \left( \frac{\partial_\theta \mathcal{J}_{\sqrt{2\mu}} \Phi}{r} \right) \partial_r f + \left( \frac{\partial_r \mathcal{J}_{\sqrt{2\mu}} \Phi}{r} \right) \partial_\theta f + \\ v \partial_z f - \left( \partial_z \mathcal{J}_{\sqrt{2\mu}} \Phi \right) \partial_v f = 0 \end{aligned} \quad (2.7)$$

for  $(r, \theta, z, v) \in [r_{\min}, r_{\max}] \times [0, 2\pi] \times [0, L] \times [-v_{\max}, v_{\max}]$ .

### 3 Method based on Padé approximations

Padé approximation is a classic way to solve numerically the quasi-neutrality equation (2.6). More precisely, we can use such an approximation in order to compute the term

$$\tilde{\Phi} = \int_{\mathbb{R}^+} \mathcal{J}_{\sqrt{2\mu T_i}}^2(\Phi) e^{-\mu} d\mu.$$

In Fourier space associated to the variable  $\theta$ , the gyroaverage is reduced to the multiplication by the Bessel function  $J_0$  of argument  $k_\perp \rho$ . Indeed, the Fourier transform of  $\mathcal{J}_\rho(f)$  can be written as

$$\begin{aligned} \widehat{\mathcal{J}_\rho(f)}(\vec{k}) &= \frac{1}{2\pi} \int_{\mathbb{R}^2} \int_0^{2\pi} f(\vec{x}_G + \vec{\rho}) d\alpha e^{-i\vec{x}_G \cdot \vec{k}} d\vec{x}_G \\ &= \frac{1}{2\pi} \int_0^{2\pi} \int_{\mathbb{R}^2} f(\vec{x}_G + \vec{\rho}) e^{-i(\vec{x}_G + \vec{\rho}) \cdot \vec{k}} d\vec{x}_G e^{i\vec{\rho} \cdot \vec{k}} d\alpha \\ &= \left( \frac{1}{2\pi} \int_0^{2\pi} e^{ik\rho \cos(\alpha - \theta)} d\alpha \right) \widehat{f}(\vec{k}) \end{aligned}$$

which leads to

$$\widehat{\mathcal{J}_\rho(f)}(\vec{k}) = J_0(k\rho) \widehat{f}(\vec{k}).$$

where  $J_0$  is the Bessel function of the first kind and of order 0. This relation implies  $\widehat{\Phi}(\mathbf{k}) = \Gamma_0(|\mathbf{k}|^2 T_i) \widehat{\Phi}(\mathbf{k})$  where the function  $\Gamma_0$  is defined by

$$\Gamma_0(k) := \int_{\mathbb{R}^+} \exp(-x^2/2) J_0^2(x\sqrt{k}) x dx.$$

Then, the left part of the quasi-neutrality equation (2.6) becomes

$$\int_{\mathbb{R}^+} (\Phi - \widehat{\mathcal{J}_{\sqrt{2\mu T_i}}^2(\Phi)}) \exp(-\mu) d\mu = (1 - \Gamma_0(|\mathbf{k}|^2 T_i)) \widehat{\Phi}.$$

Let  $I_0$  be the modified Bessel function of first kind, one can prove that  $\Gamma_0(k) = I_0(k) e^{-k}$  (see [28]).

### 3.1 classic Padé approximation

The classic Padé approximation

$$\frac{1}{1 - \Gamma_0(x)} \approx \frac{1}{x}$$

gives  $\Gamma_0(|\mathbf{k}|^2 T_i) \approx 1 - |\mathbf{k}|^2 T_i$  and using this approximation, we obtain (see [19, 11, 27]):

$$-\nabla_{\perp} \cdot (n_i \nabla_{\perp} \Phi) + \frac{n_0}{T_e} (\Phi - \langle \Phi \rangle) = \bar{n}_i - n_0.$$

A linearization of the diffusion term by assuming that  $n_i(\mathbf{x}) \approx n_0(r)$  (see [15, 19]) leads to:

$$-\nabla_{\perp} \cdot (n_0 \nabla_{\perp} \Phi) + \frac{n_0}{T_e} (\Phi - \langle \Phi \rangle) = \bar{n}_i - n_0$$

and finally:

$$-\left( \partial_r^2 \Phi + \left( \frac{1}{r} + \frac{\partial_r n_0(r)}{n_0(r)} \right) \partial_r \Phi + \frac{1}{r^2} \partial_{\theta}^2 \Phi \right) + \frac{1}{T_e} (\Phi - \langle \Phi \rangle) = \frac{1}{n_0} (\bar{n}_i - n_0).$$

This Poisson equation can be solved using FFT in  $\theta$  and finite differences in  $r$ . In the numerical results, we use centered differences of order 2 which leads to a tridiagonal system. As boundaries conditions, we consider homogeneous Neumann condition for the mode 0 and homogeneous Dirichlet condition for the other modes in  $r_{\min}$  and homogeneous Dirichlet condition for all modes in  $r_{\max}$ .

### 3.2 New Padé approximation

In the same spirit, we can increase the degree of the Padé approximation by considering a denominator of degree 2:

$$\frac{1}{1 - \Gamma_0(x)} \approx \begin{cases} \frac{-4}{3x^2 - 4x} \\ \frac{-20x - 36}{7x^2 - 36x} \end{cases}$$

These developments are not satisfactory since the denominator vanishes for a positive value ( $x = \frac{4}{3}$  for the first approximation and  $x = \frac{36}{7}$  for the second approximation). To overcome this problem, we are looking for an approximation of the form

$$\frac{1}{1 - \Gamma_0(x)} \approx \frac{ax + b}{x^2 + cx + d}$$

with  $a, b, c, d \in \mathbb{R}$ . Since  $\frac{1}{1 - \Gamma_0(x)} \xrightarrow{x \rightarrow 0} +\infty$ , we assume that  $d = 0$ . The following expansions:

$$\begin{aligned} \frac{ax + b}{x^2 + cx} &= \frac{b/c}{x} + \frac{a - b/c}{c} + \mathcal{O}(x) \\ \frac{1}{1 - \Gamma_0(x)} &= \frac{1}{x} + \frac{3}{4} + \mathcal{O}(x) \end{aligned}$$

imply  $b = c$  and  $a = \frac{3}{4}c + 1$ . Finally, by setting  $\varepsilon = 1/c$ , we obtain the following approximation:

$$\frac{1}{1 - \Gamma_0(x)} \approx \frac{1 + (\frac{3}{4} + \varepsilon)x}{x(1 + \varepsilon x)}.$$

So that the denominator does not vanish in  $\mathbb{R}_+^*$ , we impose the condition  $\varepsilon \geq 0$  and moreover  $\varepsilon > 0$  in order to damp the high frequencies. Note that this new approximation corresponds to the previous Padé approximation  $x \mapsto \frac{-20x-36}{7x^2-36x}$  with  $\varepsilon = -\frac{7}{36}$ . In Fig. 1, the function  $\frac{1}{1-\Gamma_0}$  is plotted, its classic approximation  $1/x$  and the new approximation (with  $\varepsilon = 0.1$  and  $0.001$ ) over the domain  $[0.2, 2]$ . We can see that the new Padé approximation fits better the function than the classic approximation. This new approximation gives

$$\Gamma_0(|\mathbf{k}|^2 T_i) \approx \frac{1 + (\varepsilon - \frac{1}{4})T_i|\mathbf{k}|^2 - \varepsilon T_i^2|\mathbf{k}|^4}{1 + (\frac{3}{4} + \varepsilon)T_i|\mathbf{k}|^2}.$$

Using this approximation of  $\Gamma_0$  and assuming that  $\langle \Phi \rangle = 0$ , we obtain:

$$-\varepsilon T_i^2 \Delta_\perp^2 \Phi + T_i \left[ 1 + \frac{T_i}{T_e} \left( \frac{3}{4} + \varepsilon \right) \right] \Delta_\perp \Phi - \frac{T_i}{T_e} \Phi = \left[ \left( \frac{3}{4} + \varepsilon \right) T_i \Delta_\perp - 1 \right] \frac{T_i (\bar{n}_i - n_0)}{n_0}$$

and finally:

$$-\varepsilon T_i^2 \left( \partial_r^4 + \frac{2}{r^2} \partial_r^2 \partial_\theta^2 + \frac{1}{r^4} \partial_\theta^4 + \frac{2}{r} \partial_r^3 - \frac{2}{r^3} \partial_r \partial_\theta^2 - \frac{1}{r^2} \partial_r^2 + \frac{4}{r^4} \partial_\theta^2 + \frac{1}{r^3} \partial_r \right) \Phi + T_i \left[ 1 + \frac{T_i}{T_e} \left( \frac{3}{4} + \varepsilon \right) \right] \left( \partial_r^2 + \frac{1}{r} \partial_r + \frac{1}{r^2} \partial_\theta^2 \right) \Phi - \frac{T_i}{T_e} \Phi = \left[ \left( \frac{3}{4} + \varepsilon \right) T_i \Delta_\perp - 1 \right] \frac{T_i (\bar{n}_i - n_0)}{n_0}.$$

Again, this Poisson equation can be solved using FFT in  $\theta$  and finite differences in  $r$ . In the numerical results, we use centered differences of order 2 which leads to a pentadiagonal system. As boundaries conditions, we consider homogeneous Dirichlet and homogeneous Neumann conditions in  $r_{\min}$  and  $r_{\max}$ .

## 4 Numerical method based on interpolation

We present in this part a method in the space configuration which consists in integrating on the gyrocircles using interpolation for solving the quasi-neutrality equation (2.6). This equation reads by making the change of variable  $\tilde{\mu} = \mu T_i$ :

$$\int_{\mathbb{R}^+} \left( \left( 1 + \frac{T_i}{T_e} \right) \Phi - \mathcal{J}_{\sqrt{2\tilde{\mu}}}^2(\Phi) \right) \exp\left(-\frac{\tilde{\mu}}{T_i}\right) d\tilde{\mu} = T_i^2 \frac{\bar{n}_i - n_0}{n_0}.$$

This method is directly based on the computation of the gyroaverage described in [35] which consists to interpolate the distribution function in  $N$  uniformly distributed points on the Larmor circle. To do this, we consider a uniform polar mesh on the domain  $[r_{\min}, r_{\max}] \times [0, 2\pi]$  including  $N_r \times N_\theta$  cells:

$$C_{ij} = [r_i, r_{i+1}] \times [\theta_j, \theta_{j+1}], \quad i = 0, \dots, N_r, \quad j = 0, \dots, N_\theta - 1$$

where

$$r_i = r_{\min} + i \frac{r_{\max} - r_{\min}}{N_r}, \quad i = 0, \dots, N_r,$$

$$\theta_j = j \frac{2\pi}{N_\theta}, \quad j = 0, \dots, N_\theta.$$

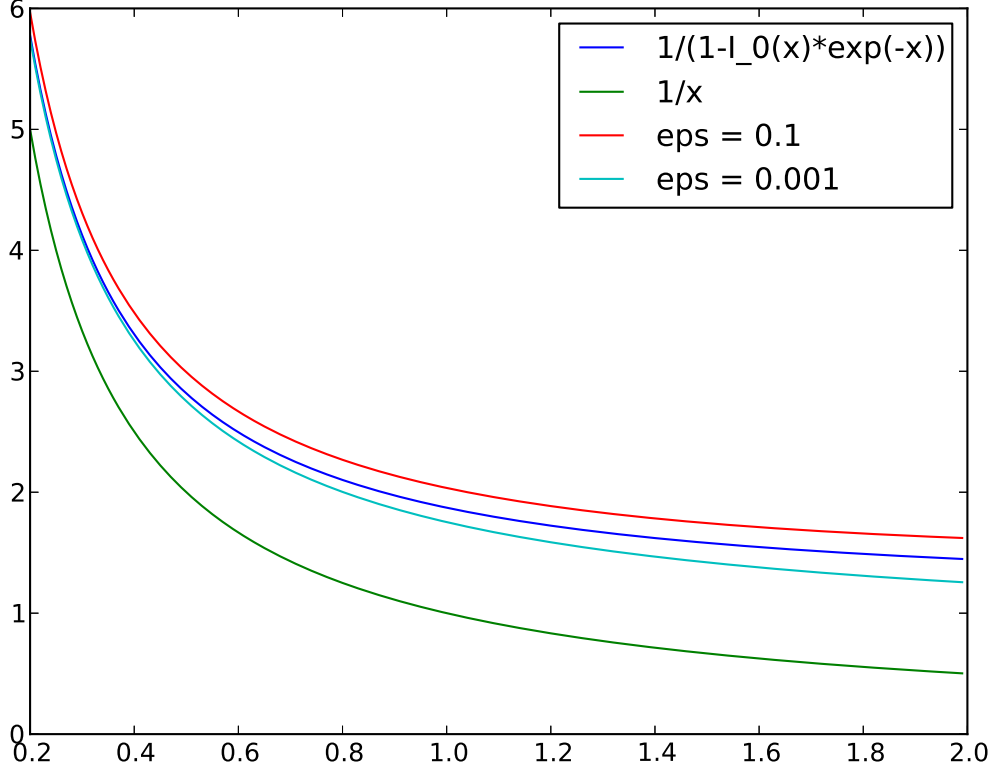


Figure 1: The function  $\frac{1}{1-\Gamma_0}$  (blue curve) compare to its classic Padé approximation  $1/x$  (green curve) and the new approximations with  $\varepsilon = 0.1$  (red curve) and  $\varepsilon = 0.001$  (cyan curve).

The computation of the gyroaverage writes, for  $(r_i, \theta_j)$  a point of the polar mesh:

$$\mathcal{J}_\rho(\Phi)(r_i, \theta_j) \simeq \frac{1}{N} \sum_{\ell=0}^{N-1} \mathcal{P}(\Phi) \left( r_i \cos(\theta_j) + \rho \cos\left(\frac{2\ell\pi}{N}\right), r_i \sin(\theta_j) + \rho \sin\left(\frac{2\ell\pi}{N}\right) \right),$$

where  $\mathcal{P}$  is an interpolation operator. In the following, we will use the cubic splines interpolation. We make a radial projection on the boundaries for the points outside the domain and we consider  $2\pi$ -periodic conditions in  $\theta$ .

In order to detail the steps of the solver, we note

$$\begin{aligned} \Phi_{i,j} &:= \Phi(r_i, \theta_j), & i = 0..N_r, j = 0..N_\theta - 1 \\ \mathcal{J}_\rho \Phi_{i,j} &:= \mathcal{J}_\rho(\Phi)(r_i, \theta_j), & i = 0..N_r, j = 0..N_\theta - 1 \\ \phi &:= {}^t(\Phi_{0,0}, \dots, \Phi_{0,N_\theta-1}, \Phi_{1,0}, \dots, \Phi_{1,N_\theta-1}, \dots, \Phi_{N_r,1}, \dots, \Phi_{N_r,N_\theta-1}) \\ \mathcal{J}_\rho(\phi) &:= {}^t(\mathcal{J}_\rho \Phi_{0,0}, \dots, \mathcal{J}_\rho \Phi_{0,N_\theta-1}, \mathcal{J}_\rho \Phi_{1,0}, \dots, \mathcal{J}_\rho \Phi_{1,N_\theta-1}, \dots, \mathcal{J}_\rho \Phi_{N_r,0}, \dots, \mathcal{J}_\rho \Phi_{N_r,N_\theta-1}). \end{aligned}$$

1. Construction of the matrix  $A^{spl} \in \mathcal{M}_{(N_r+3) \times N_\theta, (N_r+1) \times N_\theta}(\mathbb{R})$  such that  $S = A^{spl} \phi$  is the vector of splines coefficients. We consider Hermite splines with homoge-

neous Neumann boundary condition in  $r$  and periodic conditions in  $\theta$ . The matrix  $A^{spl}$  is independent of the Larmor radius.

2. For each Larmor radius  $\rho_j = \sqrt{2\tilde{\mu}_j}$ , construction of the matrix  $A_{\rho_j}^{contr} \in \mathcal{M}_{(N_r+1) \times N_\theta, (N_r+3) \times N_\theta}(\mathbb{R})$  giving the contribution of the gyroaverage of radius  $\rho_j$  in each point in function of the splines coefficients. We have also  $\mathcal{J}_{\rho_j}(\phi) = A_{\rho_j}^{contr} S$  and the matrix of the gyroaverage for the Larmor radius  $\rho_j$  is given by  $G_{\rho_j} = A_{\rho_j}^{contr} A^{spl}$ . The matrix given the double gyroaverage is obtained by  $B_{\rho_j} = G_{\rho_j}^2$ . We underline that for a given mesh in  $\rho_j$ , these matrices can be computed once for all.
3. Evaluation of the integral by quadrature in  $\tilde{\mu}$ :

$$\begin{aligned} \int_{\mathbb{R}^+} (\Phi - \mathcal{J}_{\sqrt{2\tilde{\mu}}}^2(\Phi)) e^{-\tilde{\mu}/T_i} d\tilde{\mu} &\approx \int_0^{\tilde{\mu}_{\max}} (\Phi - \mathcal{J}_{\sqrt{2\tilde{\mu}}}^2(\Phi)) e^{-\tilde{\mu}/T_i} d\tilde{\mu} \\ &\approx \sum_{j=1}^{N_\mu} c_j (\Phi - \mathcal{J}_{\sqrt{2\mu_j}}^2(\Phi)) e^{-\tilde{\mu}_j/T_i} \\ &\approx \left[ \sum_{j=1}^{N_\mu} c_j (\text{Id} - B_{\rho_j}) e^{-\tilde{\mu}_j/T_i} \right] \Phi. \end{aligned}$$

In numerical results, we use the Simpson quadrature.

4. Inversion of the matrix of the quasi-neutrality operator using LU decomposition.

*Remark 1.*

1. Note that all the previous steps are performed in precomputation.
2. An integration method is also presented in [28] based on the approximation of the function  $\Gamma_0$ .

We construct the matrix of the quasi-neutrality operator in the Fourier basis. In fact, the computation is more efficient in this basis since the matrix products, used for the construction of the double gyroaverage matrix, involve block diagonal matrix. This method was already used, for instance in [30]. More precisely, the periodicity in  $\theta$  ensures that the matrices  $A_{\rho_j}^{contr}$  and  $A^{spl}$  are block circulant:

$$\begin{aligned} A^{spl} &= \begin{pmatrix} A_0^{spl} & A_1^{spl} & \dots & A_{N_\theta-1}^{spl} \\ A_{N_\theta-1}^{spl} & \ddots & \ddots & \vdots \\ \vdots & \ddots & \ddots & A_1^{spl} \\ A_1^{spl} & \dots & A_{N_\theta-1}^{spl} & A_0^{spl} \end{pmatrix} \in \mathcal{M}_{(N_r+3) \times N_\theta, (N_r+1) \times N_\theta}(\mathbb{R}) \\ A_{\rho_j}^{contr} &= \begin{pmatrix} A_{\rho_j,0}^{contr} & A_{\rho_j,1}^{contr} & \dots & A_{\rho_j,N_\theta-1}^{contr} \\ A_{\rho_j,N_\theta-1}^{contr} & \ddots & \ddots & \vdots \\ \vdots & \ddots & \ddots & A_{\rho_j,1}^{contr} \\ A_{\rho_j,1}^{contr} & \dots & A_{\rho_j,N_\theta-1}^{contr} & A_{\rho_j,0}^{contr} \end{pmatrix} \in \mathcal{M}_{(N_r+1) \times N_\theta, (N_r+3) \times N_\theta}(\mathbb{R}) \end{aligned}$$

where  $A_i^{spl} \in \mathcal{M}_{N_r+3, N_r+1}(\mathbb{R})$  and  $A_{\rho_j, i}^{contr} \in \mathcal{M}_{N_r+1, N_r+3}(\mathbb{R})$  for  $i = 0, \dots, N_\theta - 1$ . These matrices are diagonalisable in the Fourier basis: where

$$D_{spl} = \begin{pmatrix} D_0^{spl} & & \\ & \ddots & \\ & & D_{N_\theta-1}^{spl} \end{pmatrix} \quad D_{\rho_j}^{contr} = \begin{pmatrix} D_{\rho_j, 0}^{contr} & & \\ & \ddots & \\ & & D_{\rho_j, N_\theta-1}^{contr} \end{pmatrix}$$

with

$$D_m^{spl} = \sum_{k=0}^{N_\theta-1} A_k^{spl} e^{-\frac{2i\pi km}{N_\theta}}, \quad D_{\rho_j, m}^{contr} = \sum_{k=0}^{N_\theta-1} A_{\rho_j, k}^{contr} e^{-\frac{2i\pi km}{N_\theta}}$$

and

$$U_n = \begin{pmatrix} U_{n,0,0} & \cdots & U_{n,0,N_\theta-1} \\ \vdots & \ddots & \vdots \\ U_{n,N_\theta-1,0} & \cdots & U_{n,N_\theta-1,N_\theta-1} \end{pmatrix}, \quad U_{n,k,\ell} = \frac{1}{\sqrt{N_\theta}} e^{\frac{2i\pi k\ell}{N_\theta}} I_n$$

where  $I_n$  is the identity matrix of size  $n \times n$ .

The advantage of the diagonalisation in the Fourier basis is that the computation of the gyroaverage of  $\Phi$  by the product  $G G_{\rho_j} \Phi$  can be performed using a fast algorithm:

1. Change to Fourier basis by FFT( $\Phi$ ).
2. Computation of the product  $G_{\rho_j} \Phi$  in the Fourier basis.
3. Change to real space by FFT<sup>-1</sup> of the previous result.

The use of polar mesh and FFT allow to make more quickly computations and provides a base for a future work in more complex geometry.

## 5 Numerical results

To deal with the equation system (2.6)-(2.7), we have used the SELALIB platform [34] with a classic semi-Lagrangian method with cubic splines interpolation, predictor corrector method and Verlet algorithm for the characteristics. In our case the MPI parallelization is based on transpositions between  $(r, \theta, v)$  domain decomposition and  $z$  domain decomposition.

In the simulations, we will take  $\lambda = 0$  (no zonal flow case). The initial distribution function reads:

$$f(0, r, \theta, z, v) = f_{eq}(r, v) \times \left( 1 + \varepsilon \exp\left(-\frac{(r-r_p)^2}{\delta r}\right) \cos\left(\frac{2\pi n}{L}z + m\theta\right) \right)$$

where the equilibrium function  $f_{eq}$  is

$$f_{eq}(r, v) = \frac{n_0(r) \exp\left(-\frac{v^2}{2T_i(r)}\right)}{(2\pi T_i(r))^{1/2}}.$$

The profiles  $T_i, T_e$  and  $n_0$  are given by:

$$\mathcal{P}(r) = C_{\mathcal{P}} \exp\left(-\kappa_{\mathcal{P}} \delta r_{\mathcal{P}} \tanh\left(\frac{r-r_p}{\delta r_{\mathcal{P}}}\right)\right)$$

where  $\mathcal{P} \in \{T_i, T_e, n_0\}$ ,  $C_{T_i} = C_{T_e} = 1$  and

$$C_{n_0} = \frac{r_{\max} - r_{\min}}{\int_{r_{\max}}^{r_{\min}} \exp\left(-\kappa_{n_0} \delta r_{n_0} \tanh\left(\frac{r-r_p}{\delta r_{n_0}}\right)\right) dr}.$$

We consider the parameters of [6] [Medium case]:

$$\begin{aligned} r_{\min} &= 0.1, r_{\max} = 14.5, v_{\max} = 7.32, \kappa_{n_0} = 0.055, \\ \kappa_{T_i} &= \kappa_{T_e} = 0.27586, \delta r_{T_i} = \delta r_{T_e} = \frac{\delta r_{n_0}}{2} = 1.45, \\ \varepsilon &= 10^{-6}, n = 1, m = 5, \\ L &= 1506.759067, r_p = \frac{r_{\min} + r_{\max}}{2}, \delta_r = \frac{4\delta r_{n_0}}{\delta r_{T_i}}. \end{aligned}$$

We compare the performance of the different numerical methods for the quasi-neutrality operator on the machines:

- IRMA-HPC2 with the parameters:  $64 \times 64 \times 32 \times 64$ ,  $\Delta t = 5$ , 1000 iterations.
- CURIE with the parameters:  $128 \times 256 \times 32 \times 128$ ,  $\Delta t = 2$ , 4000 iterations.

For the right side of the quasi-neutrality equation, we use the Hermite interpolation method in order to compute the gyroaverage (see [35]) using 1024 points on the Larmor circle with  $\mu = 0.7$  on IRMA-HPC2 and  $\mu = 1$  on CURIE.

The numerical and performance results are given in Table 1, Fig. 2 and Fig. 3. In Table 1, we see that the new Padé approximation is slower than the classic one but faster than the interpolation method. The performance results of the interpolation method seem to be only slightly affected by the number of quadrature points in  $\mu$ . Indeed, the steps involving the quadrature in  $\mu$  and the construction of the double gyroaverage matrix are performed once for all in precomputation. The Fig. 2 and 3 show that the instability rate obtained with the new Padé approximation is higher than the instability rate obtained with the classical Padé, this is in agreement with Fig. 1. Moreover, the instability rate obtained by the interpolation method is also higher than the instability rate obtained with the classical Padé, this is the opposite behavior of the simple gyroaverage case but there is no compensation in general. The rate of the new Padé method converges to the rate obtained with the interpolation method and we observe that these 2 methods give similar results in Fig. 2 and reveal small structures in the non-linear phase which are not present with the classic Padé method. For memory limitation reasons, we cannot take more than 33 quadrature points in  $\mu$  on CURIE. An outlook would be to make a parallelization in  $\mu$  in order to increase this number of quadrature points.

		Interpolation		
Classic Padé	New Padé	$N_\mu = 9$	$N_\mu = 17$	$N_\mu = 33$
70490	73281	75258	75271	75311

Table 1: Execution time (in s.) on CURIE with 32 processors. Parameters:  $128 \times 256 \times 32 \times 128$ ,  $\Delta t = 2$ , 4000 iterations.

## Conclusion

We have validated two new methods on polar geometry for solving the quasi-neutrality equation. Comparisons are made with classic Padé approximation, considering a  $4D$  drift-kinetic model with one fixed Larmor radius for the distribution function and an integration in  $\mu$  for the potential. We find that the instability rate obtained by the new Padé approximation is closer to the rate obtained by the interpolation method (which is accurate when the number of quadrature points increases) than for the classic Padé approximation which is smaller. This is a preliminary study; further study in GYSELA is envisioned.

## References

- [1] M. ABRAMOWITZ, I. A. STEGUN, *Handbook of Mathematical Functions*, (Dover Publications, New York, 1965).
- [2] N. BESSE, P. BERTRAND, *Gyro-water-bag approach in nonlinear gyrokinetic turbulence*, J. Comput. Phys. **228** (2009), pp. 3973–3995.
- [3] M. BOSTAN, *Transport equations with disparate advection fields. Application to the gyrokinetic models in plasmas physics*, J. Differential Equations **249** (2010) pp. 1620–1663.
- [4] J.-P. BRAEUNIG, N. CROUSEILLES, V. GRANDGIRARD, G. LATU, M. MEHRENBARGER, E. SONNENDRÜCKER *Some numerical aspects of the conservative PSM scheme in a 4D drift-kinetic code*. Research report INRIA (2009).
- [5] A. BRIZARD, *Nonlinear gyrokinetic Maxwell-Vlasov equations using magnetic coordinates*, J. Plasma Phys. **41** (1989), pp. 541–559.
- [6] D. COULETTE, N. BESSE, *Numerical comparisons of gyrokinetic multi-water-bag models*. JCP **248** (2013), pp. 1–32.
- [7] N. CROUSEILLES, P. GLANC, S. HIRSTOAGA, E. MADAULE, M. MEHRENBARGER, J. PÉTRI, *Semi-Lagrangian simulations on polar grids: from diocotron instability to ITG turbulence*, Eur. Phys. J. D **68** (2014), p. 252.  
DOI: 10.1140/epjd/e2014-50180-9
- [8] N. CROUSEILLES, M. MEHRENBARGER, H. SELLAMA, *Numerical solution of the gyroaverage operator for the finite gyroradius guiding-center model*, CiCP **8** (2010), pp. 484–510.
- [9] N. CROUSEILLES, A. RATNANI, E. SONNENDRÜCKER, *An Isogeometric Analysis Approach for the study of the gyrokinetic quasi-neutrality equation*, Journal of Computational Physics **231**, No. 2 (2012), pp. 373–393.
- [10] A. DIMITS et al., *Comparisons and physics basis of tokamak transport models and turbulence simulations*, Physics of Plasmas **7**, No. 3 (2000), pp. 969–983.
- [11] D.H.E. DUBIN, J. A. KROMMES, C. OBERMAN, W. W. LEE, *Nonlinear gyrokinetic equations*, Phys. Fluids **26**, No. 12 (1983).
- [12] F. FILBET, C. YANG, *Conservative and non-conservative methods based on Hermite weighted essentially-non-oscillatory reconstruction for Vlasov equations*, J. Comput. Physics, **279** (2014).
- [13] F. FILBET, C. YANG, *Mixed semi-Lagrangian/finite difference methods for plasma simulations*, submitted.
- [14] X. GARBET, Y. IDOMURA, L. VILLARD, T.H. WATANABE, *Gyrokinetic simulations of turbulent transport*, Nuclear Fusion **50**, No. 4 (2010), 043002.
- [15] V. GRANDGIRARD, M. BRUNETTI, P. BERTRAND, N. BESSE, X. GARBET, P. GHENDRIH, G. MANFREDI, Y. SARAZIN, O. SAUTER, E. SONNENDRÜCKER, J. VACLAVIK, L. VILLARD, *A drift-kinetic Semi-Lagrangian 4D code for ion turbulence simulation*. J. Comput. Physics, **217**, No. 2 (2006), pp. 395–423.
- [16] V. GRANDGIRARD, Y. SARAZIN, X. GARBET, G. DIF-PRADALIER, Ph. GHENDRIH, N. CROUSEILLES, G. LATU, E. SONNENDRÜCKER, N. BESSE, P. BERTRAND, *Computing ITG turbulence with a full-f semi-Lagrangian code*, Communications in Nonlinear Science and Numerical Simulation **13** No. 1 (2008), pp. 81–87.

- [17] T. GÖRLER, *Multiscale effects in plasma microturbulence*, PhD thesis, Ulm (2009).
- [18] T. GÖRLER, X. LAPILLONNE, S. BRUNNER, T. DANNERT, F. JENKO, F. MERZ, D. TOLD, *The global version of the gyrokinetic turbulence code GENE*, J. Comput. Physics **230**, No. 18 (2011), pp. 7053–7071.
- [19] T.S. HAHM, *Nonlinear Gyrokinetic Equations for Tokamaks Microturbulence*, Phys. of Fluids **31** (1988).
- [20] R. HATZKY, T.M. TRAN, A. KONIES, R. KLEIBER, S.J. ALLFREY, *Energy conservation in a nonlinear gyrokinetic particle-in-cell code for ion-temperature-gradient-driven modes in theta-pinch geometry*, Physics of Plasmas **9**, No. 3 (2002), pp. 898–912.
- [21] M. HAURAY, A. NOURI, Ph. GHENDRIH, *Derivation of a gyrokinetic model: existence and uniqueness of specific stationary solutions*, KRM **4** (2009), pp. 707–725.
- [22] Y. IDOMURA, S. TOKUDA, Y. KISHIMOTO, M. WAKATANI, *Gyrokinetic theory of drift waves in negative shear tokamaks*, Nuclear Fusion **41**, No. 4 (2001).
- [23] S. JOLLIET, A. BOTTINO, P. ANGELINO, R. HATZKY, T.M. TRAN, B.F. MCMILLAN, O. SAUTER, K. APPERT, Y. IDOMURA, L. VILLARD, *A global collisionless PIC code in magnetic coordinates*, Comp. Phys. Comm. **177**, No. 5 (2007), pp. 409–425.
- [24] R. KLEIN, E. GRAVIER, P. MOREL, N. BESSE, P. BERTRAND *Gyrokinetic waterbag modeling of a plasma column: Magnetic moment distribution and finite Larmor radius effects*, Physics of plasmas **16**, 082106 (2009).
- [25] M. KREH, *Bessel Functions*, [www.math.psu.edu/papikian/Kreh.pdf](http://www.math.psu.edu/papikian/Kreh.pdf)
- [26] W. W. LEE, *Gyrokinetic approach in particle simulation*, Physics of Fluids **26**, No. 2 (1983), pp. 556–562.
- [27] W.W. LEE, R.A. KOLESNIKOV, *On higher-order corrections to gyrokinetic Vlasov-Poisson equations in the long wavelength limit*, Phys. of Plasmas **16**, 044506 (2009).
- [28] Z. LIN, W.W. LEE, *Method for solving the gyrokinetic Poisson equation in general geometry*, Phys. Rev. E **52** (1995), pp. 5646–5652.
- [29] G. MANFREDI, M. SHOUCRI, R.O. DENDY, A. GHIZZO, P. BERTRAND, *Vlasov gyrokinetic simulations of ion-temperature-gradient driven instabilities*, Physics of Plasmas. **3**, No. 202 (1996), pp. 202–217.
- [30] M. MEHRENBERGER, C. STEINER, L. MARRADI, N. CROUSEILLES, E. SONNENDRÜCKER, B. AFEYAN, *Vlasov on GPU*, ESAIM Proc., 2013.
- [31] A. MISHCHENKO, A. KNIES, R. HATZKY, *Particle simulations with a generalized gyrokinetic solver*, Phys. of Plasmas **12**, 062305 (2005).
- [32] M. SHOUCRI, G. MANFREDI, P. BERTRAND, A. GHIZZO, J. LEBAS, G. KNORR, *Charge-separation velocity shear and suppression of turbulence at a plasma edge in the gyrokinetic approximation*, Journal of Plasma Physics **61**, No. 2 (1999), pp. 191–212.
- [33] Y. SARAZIN, V. GRANDGIRARD, E. FLEURENCE, X. GARBET, Ph. GHENDRIH, P. BERTRAND, G. DEPRET, *Kinetic features of interchange turbulence*, Plasma Phys. Control. Fusion **47**, No. 10 (2005), pp. 1817–1840.
- [34] SELALIB, <http://selalib.gforge.inria.fr/>

- [35] C. STEINER, M. MEHREBERGER, N. CROUSEILLES, V. GRANDGIRARD, G. LATU, F. ROZAR, *Gyroaverage operator for a polar mesh*, Eur. Phys. J. D, 69 1, p. 18, (2015).
- [36] J.M. DE VILLIERS, C.H. ROHWER, *Optimal local spline interpolants*, Journal of Computational and Applied Mathematics **18**, No. 1 (1987), pp. 107–119.

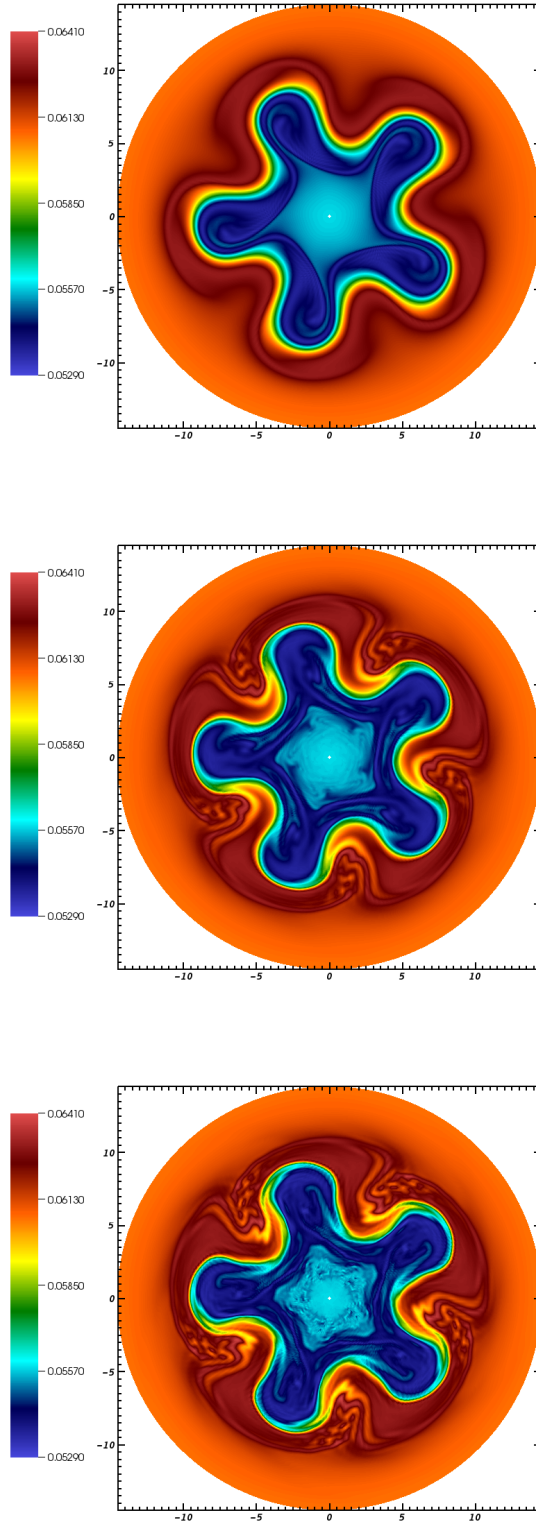


Figure 2: Poloidal cut  $f(r, \theta, 0, 0)$  at time  $T = 8000$  for  $128 \times 256 \times 32 \times 128$ ,  $\Delta t = 2$ ,  $\mu = 1$ . From top to bottom: classic Padé, new Padé ( $\varepsilon = 0.001$ ), interpolation ( $N_\mu = 33$ ) . On CURIE.

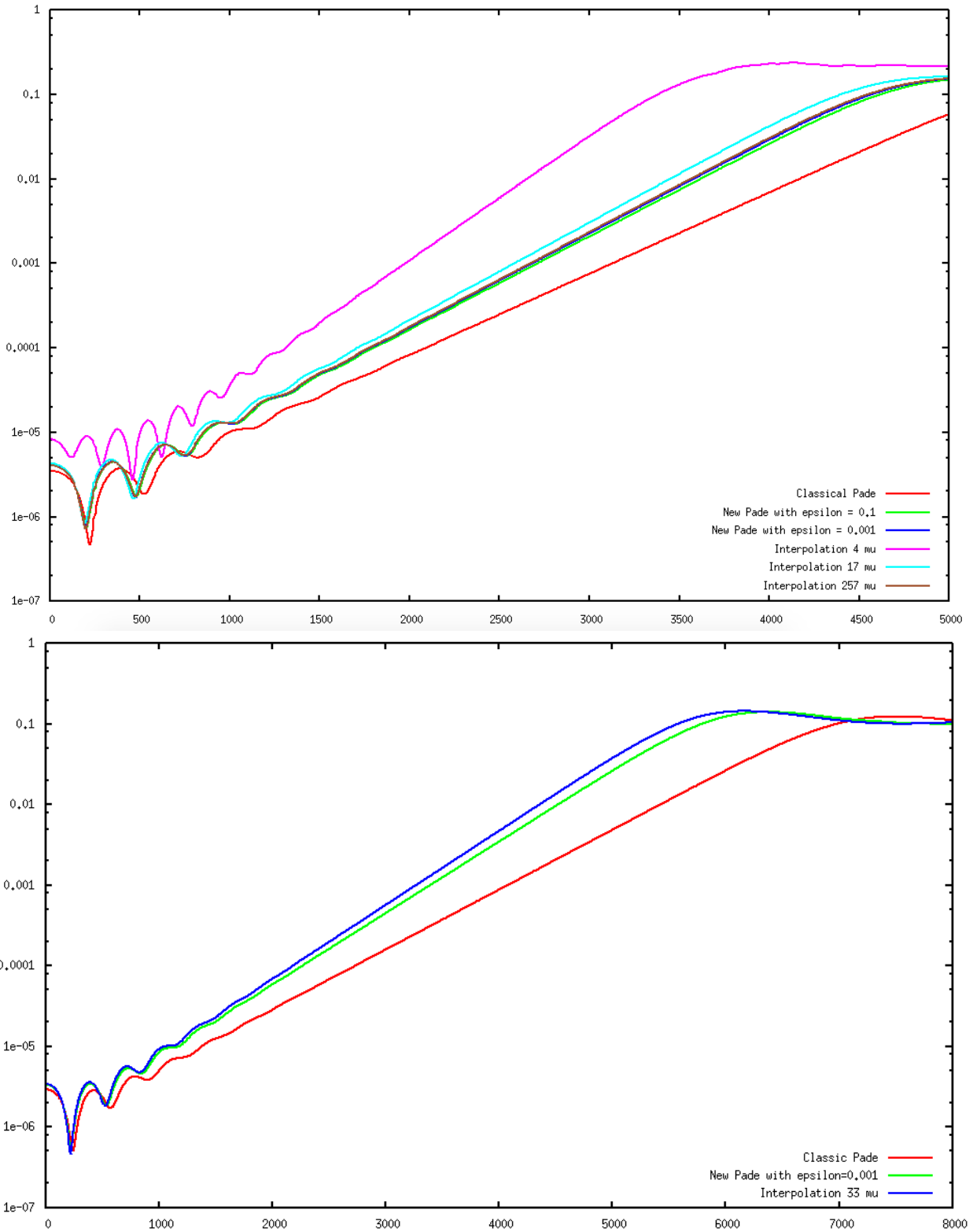


Figure 3: Time evolution of  $\int_{r_{\min}}^{r_{\max}} \int_0^{2\pi} \Phi(r, \theta, 0) r dr d\theta$  on IRMA-HPC2 with  $\mu = 0.7$  (top) and on CURIE with  $\mu = 1$  (bottom).